Spectroscopic and Microscopic Evaluation of Immobilized Cytochrome C Interaction with Cyanide/Arsenic Ligands in Quantitative Analysis

Xolile Fuku, Boitumelo Kgarebe, Emmanuel Iwuoha, Priscilla Baker

SensorLab, Department of Chemistry,
University of the Western Cape, Private Bag X17, Bellville, 7535, South Africa,
e-mail: pbaker@uwc.ac.za

The electrochemical, spectroscopic and microscopic analyses of cytochrome *c* and its immobilization on bare glassy carbon (GC) and platinum (Pt) electrodes were performed. Cytochrome *c* interaction was examined by studying cyanide and arsenic as model compounds for these types of behavior. Subtractively normalized interfacial Fourier transform infrared (SNIFTIR) spectroscopy, fluorescence and electrochemical methods, Fourier transform infrared (FTIR) spectroscopy and atomic force microscopy (AFM) were used to characterize the protein in the immobilized state and to confirm that the protein was not denatured upon binding to the pre-treated bare GC and Pt electrodes. The spherical morphology of the immobilized protein, which is typical of native cytochrome *c*, was observed using AFM. The protein binding was monitored as a decrease in peak currents (by CV) for the immobilized protein. Under analysis was also a decrease in emission intensities by fluorescence in solution, by the FTIR and SNIFTIR spectroscopies. Fluorescence and AFM proved the existence of the binding process between the protein and the analytes. This behavior was confirmed by the FTIR and SNIFTIR spectroscopies, which gave evidence that the binding event took place at the amino acids side chain of the protein.

Keywords: toxicity, cytochrome c, platinum electrode, glassy carbon electrode.

УДК 661:543.68

INTRODUCTION

Understanding the orientation, functionality and conformation of proteins on solid surfaces (e.g., electrodes) and in solutions is important in the design of biomaterials, biosensors, and bioanalytical systems. Cytochrome *c* (*cyt c*) is a relatively simple metalloprotein comprising only 104 amino acids (*1*). It is a very basic redox metalloprotein with an over charge of +7/+8 at neutral pH (*2*). *Cyt c* is also known as an electron-carrying protein (*3*). The electron shuttling function of the protein may be disrupted due to interference by arsenic and cyanide compounds. As a result, its structural nature may also be changed (*4*).

The analysis of this protein using spectroscopic methods such as Subtractively Normalized Interfacial Fourier Transform Infrared (SNIFTIR) and fluorescence, as well as microscopic (AFM) and electrochemical methods – cyclic voltammetry (CV) and squarewave voltammetry (SWV), is a very attractive approach because these techniques are highly sensitive and have long-term reliability and reproducibility and have high resolution. The spectroscopic and microscopic structural analysis of this metalloprotein has been reported, using gold and graphite electrodes (*5*). Boussaad and collaborators investigated the horse heart *cyt c* adsorption and its electrochemistry on graphite electrodes using *in situ* atomic force microscopic measurements (AFM) (*6*). Hobara and co-workers reported a scanning tunneling microscopic (STM) study on the preferential adsorption of *cyt c* on the mixed SAMs from 3-mercaptopropionic acid and 1-hexadecanethiol on Au-(111), and electrochemistry (EC) of *cyt c* molecules immobilized either electrostatically or covalently on a series of carboxy-terminated alkanethiol monolayers (*7*). More recently, specific interactions among the surface attached *cyt c,* DNA molecules and surfactants (*8*) have been studied including AFM imaging (*9*). Further, *cyt c* from yeast has been chemisorbed on bare gold electrodes and its *in situ* imaging by AFM and STM was accomplished by Bonanni with collaborators (10). Robert et al., studied the UV and resonance Raman spectra of *cyt c* conformational states (*11, 12*). SNIFTIR of *cyt c* immobilized at a Pt electrode and its spherical morphology using scanning electron microscopy (SEM) has been studied by Fuku and others (*2*, *18*). *Cyt c* has also been studied extensively in bioelectronic-based devices including biofuel cells. Choi, Oh, and others investigated a bioelectronic device consisting of a protein-adsorbed hetero-Langmuir–Blodgett (LB), in which four kinds of functional molecules – *cyt c*, viologen, flavin, and ferrocene were used as a secondary electron acceptor (A2), a first electron acceptor (A1), a sensitizer (*S*), and an electron donor (*D*), respectively (*13, 14*). They also verified photodiode characteristics of the proposed bio-electronic device, and the proposed molecular

array mimicking the photosynthetic reaction center was considered to be useful if applied as a model system for the development of a bio-molecular photodiode. Optimising the synthesis, polymer membrane encapsulation and photoreduction performance of Ru(II)- and Ir(III)-bis(terpyridine) cytochrome *c* bioconjugates was studied by David et al. (*15*). Ramanavicius and others, evaluated newly designed biofuel cells by using the efficiency of both anode and cathode that were significantly advanced by phenanthroline derivatives, which served as redox mediators (*16, 17*).

The aim of the present work was to study the structural conformation and re-orientation of *cyt c* as a result of As^{3+}/CN^- ligand binding when *cyt c* was immobilized at GC and Pt electrodes. To determine the mechanism of the protein binding at the electrode interface, the investigations of *cyt c* interaction by electrochemical, microscopic and spectroscopic methods were carried out.

EXPERIMENTAL PROCEDURES

Reagents and materials

The horse heart *cyt c* (Type I, product no. 105201), arsenic trioxide (product no. 20267) and potassium cyanide (product no. 60178) were purchased from Sigma-Aldrich. Phosphate buffer solution (PBS), 0.1M, pH 7.0, was prepared from anhydrous disodium hydrogen phosphate (Na_2HPO_4) and sodium dihydrogen phosphate (NaH_2PO_4). Deionized water (18.2 MΩ) purified by a milli-QTM system (Millipore) was used for aqueous solution preparations. Analytically graded argon (Afrox, South Africa) was used to degas the system. Sodium hydroxide (99.9%) and hydrochloric acid (75%) used in experiments were also purchased from Sigma-Aldrich. All chemicals were of analytical grade.

Apparatus and electrode preparation

Apparatus

Electrochemical experiments were performed using BAS100W Bioanalytical System (Model No: 100B). The three-electrode electrochemical cell comprised a platinum wire counter electrode, an Ag|AgCl (3M) reference electrode and a Pt or GC working electrode (3 mm in thickness and 0.07 in diameter). Fourier Transform Infrared Spectroscopy (FTIR) experiments were performed on a Perkin Elmer spectrometer – Spectrum 100; SNIFTIR experiments were performed using MISE-PS/09/ Vertex 80v, AFM experiments – 90-24OVAC, fluorescence experiments – FL3-2IHR.

Electrode preparation

The Pt and GC electrodes were cleaned using pads and Al_2O_3 powder of different sizes (1 μm, 0.3 μm, and 0.05 μm) then rinsed with distilled water. After that the electrodes were sonicated in water and ethanol. This method of cleaning was necessary to remove surface impurities and ensure good electrochemical performance of the electrodes.

Electrochemical measurements

The electrodes used for the construction of a biosensor were a reference electrode (3M, Ag/AgCl), a platinum wire (which was our counter electrode), as well as Pt and GC electrodes used as working electrodes. Incubation was used in the preparation of a biosensor, after cleaning the electrodes. GC (3 mm) electrode was incubated in 4.06×10^{-4} M *cyt c* after cleaning and activation. After preparation of the biosensor, the protein modified GC electrode was transferred to a 50-mL spectro-chemical cell and 3 mL electrochemical cell containing 0.1 M pH 7.0 PBS, before the respective measurements were made. Cyclic voltammetry was carried out to observe the redox chemistry of the protein. SNFTIR experiments were carried out to determine the formation and deformation of the bonds vibrations during oxidation and reduction of the protein. FTIR was used for confirmation of the immobilisation of *Cyt c* on Pt and GC electrode. The protein was immobilized by drop coating 10 μl *cyt c* onto bare electrodes. The electrodes were left for 2hrs to dry prior to AFM analyses (before and after applying the potential). Fluorescence measurements were carried out to determine the three-dimensional, excitation and emission fluorescence spectra using Nanolog (FL3-2IHR). The excitation and emission slits were set at 5 nm, and both excitation and emission were scanned in 5 nm intervals at 12000 nm/min.

RESULTS AND DISCUSSION

Characterisation of cyt c using AFM

AFM analyses for GC/*cyt c*, Pt/*cyt c* and bare GC and Pt electrodes were carried out using a non-contact mode cantilever. The roughness of the bare electrode surface was found to range from 4–13 nm, for both of the electrodes (Fig. 3). The modified electrodes showed clear images of the globular structure of the protein *cyt c* (Fig. 1c and e).

Figure 1 shows AFM images of GC and Pt electrodes: (a) before modification (b) after immobilization of cytochrome *c*, and (c) – after analyte binding. The surface roughness of GC is observed to be consistently higher than that of Pt. Images in Fig. 1c and e indicate that the protein is adsorbed on both GC and Pt electrodes, forming a rather thin uniform monolayer. These results agree well with those obtained by Boussaad et al. (*6*). The protein adsorbed onto GC electrode shows the globular morphology with higher surface roughness. The Pt coated elec-

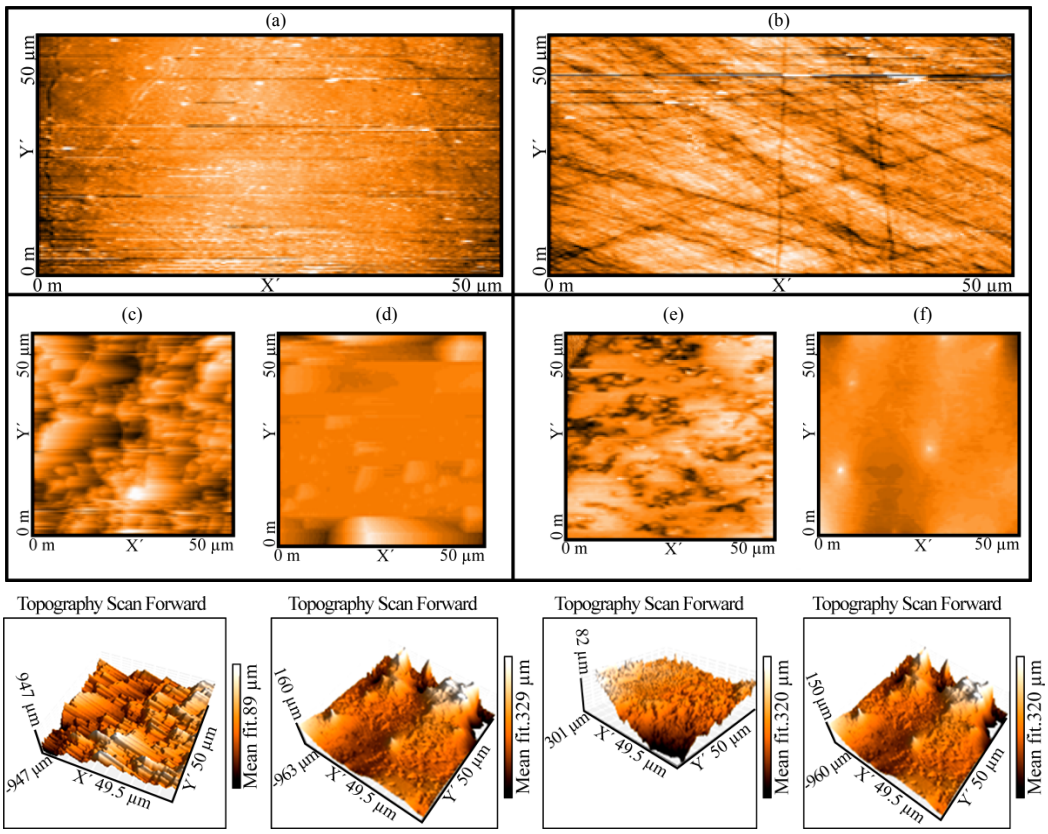

Fig. 1. AFM images of: (a) – bare GC electrode; (b) – bare Pt electrode; (c), (e) – Pt/*cyt c* and GC/*cyt c* before, and (d), (f) – Pt/*cyt c* and GC/*cyt c* after application of biosensor to KCN by cycling the potential at +600 mV to -600 mV (vs. Ag/AgCl).

trode appeared smoother than the GC coated electrode. 3D images clearly demonstrate homogeneity in roughness of the coated electrodes. Cytochrome *c* biosensors on Pt and GC electrodes became very similar in morphology after application of the biosensor to KCN. The images in Fig. 1d and f showed no visible globular morphology of *cyt c* as compared to those in Fig. 1c and e. These observations confirm the analyte adsorption onto the immobilized protein. The absorption of the analyte to the protein resulted in the analyte masking the protein thus showing no globular distribution of *cyt c* on the electrodes.

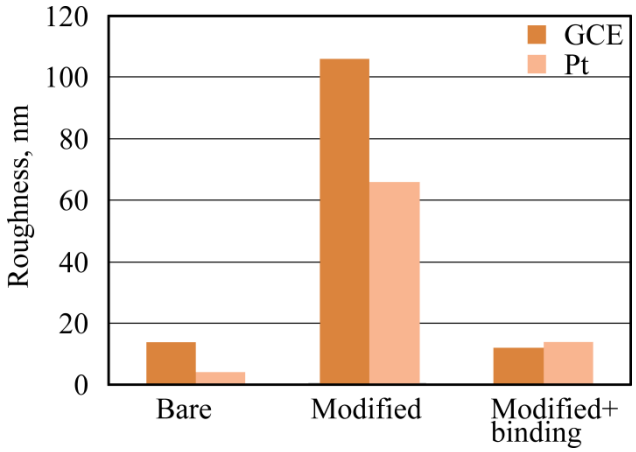

Fig. 2. Roughness estimated from AFM on bare and modified electrodes (GC and Pt).

The roughness (Ra^{-}) of the electrode immobilized with *cyt c* before applying a potential was found to range from 66–109 nm for both the Pt and GC electrodes (Fig. 2). After adsorption of the analyte the roughness was found to be between 12–13 nm. These observations suggest that *cyt c* molecules retain their globular structure before a potential was applied and lose their structural morphology after electrochemical analyses. The roughness of the modified electrode was found to be higher than that of the bare electrode, as expected. The bar plots in Fig. 2 are found to be comparative with the roughness plots acquired (Fig. 1). The images obtained here are in good agreement with the work of Boussaad et al. [6] who used a gold electrode.

Fluorescence spectroscopy

Cyt c type 1 structural changes in solution were evaluated using fluorescence measurements. The protein was dissolved in 0.1M PBs pH 7 to give a concentration of 2 µM. Flourescence of dilute solutions of the protein were measured, with spectra acquired after every 0.2 seconds. Flourescence was also used to confirm the binding of cyanide and arsenic compounds to the protein in solution. The spectra were acquired before and after successive additions of the respective analytes, i.e. cyanide and arsenic compounds (Fig. 3).

In our earlier work UV/Vis analysis of the protein was carried out before and after additions of the each analyte and the change in absorbance for the identifying peak at 409–410 nm, was measured (*18*).

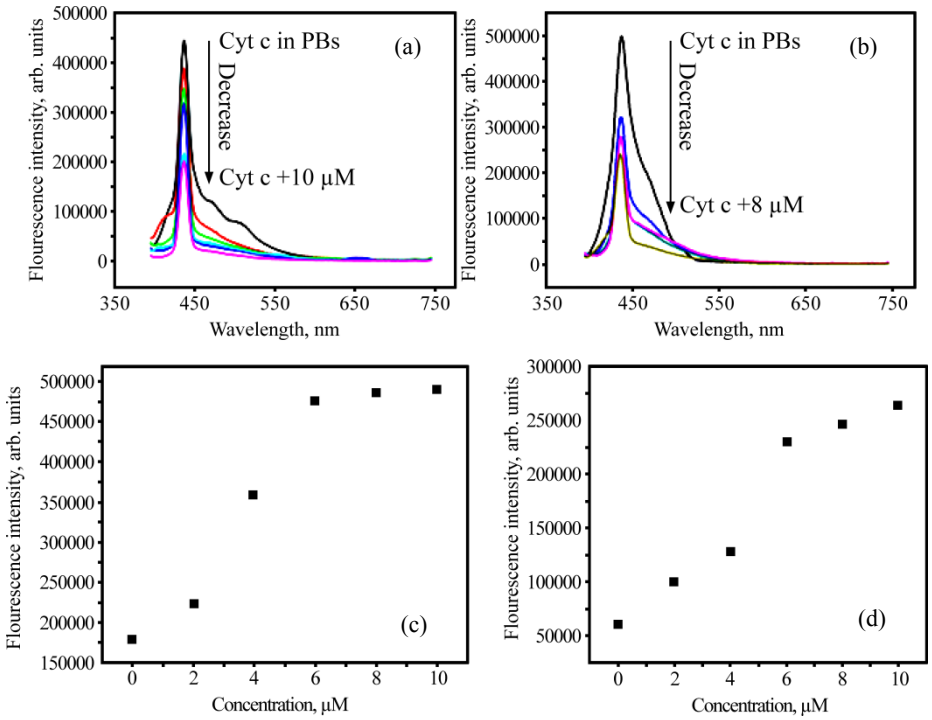

Fig. 3. (a), (b) – fluorescence emission spectra of *cyt c* after additions of cyanide and arsenic compounds; (c), (d) – calibration plots of *cyt c* response to analytes.

Cytochrome *c* exhibited an emission maximum at 430 nm. However the shift in wavelengths between the two techniques is significantly small. This shift can be related to Stokes-shift, which is longer in wavelength than the radiation that caused the excitation. Figure 3a and b shows the binding event of cyanide and arsenic compounds to protein. A decrease in fluorescence intensity as a function of increasing concentration of the each analyte, was observed. Cyanide and arsenic ligands interact with the protein, thus causing a decrease in peak intensities of the protein. This decrease in peak intensities serves as evidence of the analyte binding. Figure 3c and d shows calibration plots of *cyt c* in the presence of analyte. As we increase the concentration of the analyte the absorbance due to analyte-protein complex also increased (Fig. 3c and d), due to changes in the protein structure. This change in the protein structure is attributed to binding of CN^-/As^{3+} ligands. Through chemical reaction these ligands bind to the amino acids of the protein not to the iron, as proven in our earlier work (*18*), thus causing a change in protein electronic environment. The observed results fully agree with our UV/Vis analysis in our earlier work (*18*) and the results obtained by Zhao et al., (*28*). Similar findings were observed by Hart et al. (*19*).

Florescence analysis data for *cyt c* in 0.1M PBs pH 7 are depicted in Fig. 4. Figure 4a shows 3D analysis of the protein and in Fig. 4b and d there are plots of *cyt c* excitation and emission signals. The protein was shown (*18*) to emit at the wavelength of 430 nm, whereas here it is shown to excite at a lower wavelength – of 370 nm. The energy of the emitted (430 nm) and excited (370 nm) molecule was calculated using the following equation: $E = hc/\lambda$, where E is the energy of the molecule in J, h is Planck's constant (6.63×10^{-34} J.s), c is the speed of light in cm s^{-1} and λ is the wavelength in nm. The energy was calculated to be 1.54×10^{-28} J for emission and 5.38×10^{-28} J for excitation. The calculated values suggest that when the protein absorbs a photon it gains energy and enters an excited state (S1 = higher energy levels). One way for the molecule to relax is to emit a photon, thus losing its energy (S0 = lower energy level). When the emitted photon has less energy than the absorbed photon, as observed, this energy difference is the Stokes shift. The two wavelengths are blue shifted by 60 nm. Three-dimensional fluorescence spectra of *cyt c* are given in Fig. 4a and c. The contour plots show the *cyt c* emission maximum at 430 nm, and an excitation maximum at 370 nm, which are due to protein porphyrin ring. At least two distinct fluorophores are present in the plots. The emission is blue-shifted relative to the *cyt c* spectrum, with a maximum at 430 nm. The excitation maximum is also blue-shifted, peaking at 370 nm. Molecules with similar fluorescence maxima include several *cyt c* amino acids: i.e. tyrosine (300 nm), tryptophan (350 nm) and Met-80 residues. One of these amino acids is the fluorophore responsible for the second peak observed in the contour plots in Fig. 4a and c. Esteve-Núñez (*20*) and Chou et al., (*21*) have earlier determined the fluorescent properties of *c*-type cytochromes by revealing their potential role as an extra-

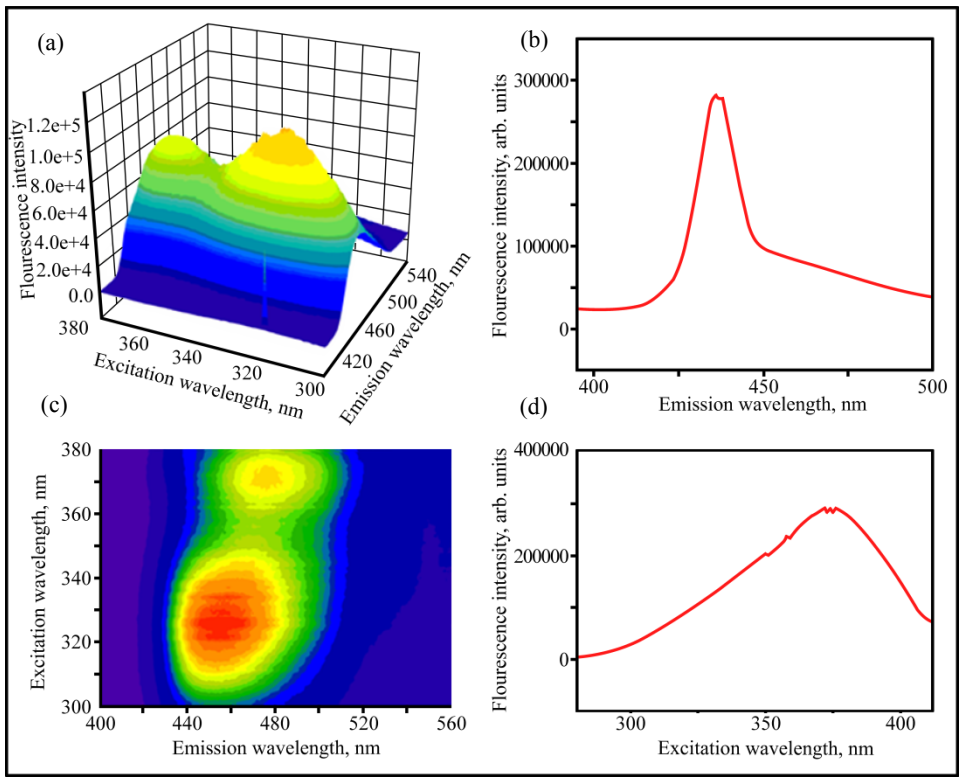

Fig. 4. (a), (c) – fluorescence spectra of – *cyt c* 3D contour plots; (b), (d) – *cyt c* emission and excitation.

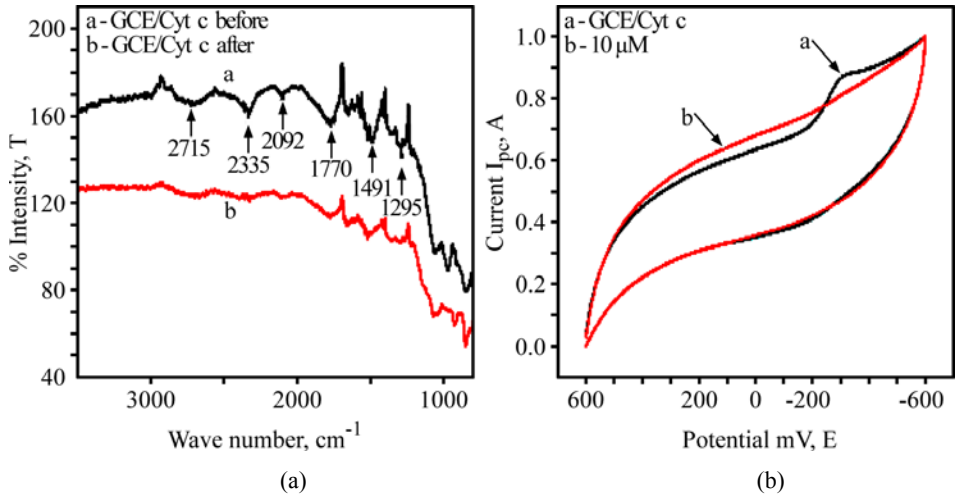

Fig. 5. (a) – FTIR spectra for *cyt c* before and after electrochemical analysis; (b) – biosensor response to As_2SO_3 (10 µM) in 0.1M PBS (pH = 7) at 25 mV s^{-1}.

cytoplasmic electron sink in *Geobacter sulphur reducens*.

FTIR and SNIFTIR spectroscopy

FTIR spectroscopy

FTIR spectroscopy was used to identify the functional groups of *cyt c*. The protein was drop coated onto the GC electrode and was dried with argon gas for 2hrs before FTIR analysis. After drying the electrode, FTIR analyses were carried out (Fig. 5a). The electrode was then used for electrochemical analysis before further analysis of FTIR (Fig. 5b).

FTIR analyses for the protein were carried out before and after the electrochemical analysis of *cyt c*. The functional groups or vibrational bands were observed as in Fig. 5a. The vibrational bands of the back-bone protein confirmed the functionality of the protein. The bands observed at 2715 cm^{-1} are due to C-H and S-H stretches, at 2335–2092 C≡N, 1770–1491 cm^{-1} C=O, C=C and C=N. Modified working electrodes (Pt/GC) in a 3 ml electrochemical cell was used for CV measurements, after which further analyses using FTIR were carried out. The spectra obtained before and after electrochemical analysis were found to have the same bands, but with lower band intensities observed after electrochemical analyses (Fig. 5a). The decrease in the spectral intensity indicates a change in the structural orientation of the protein, which results from analyte binding to the protein (Fig. 5a and b).

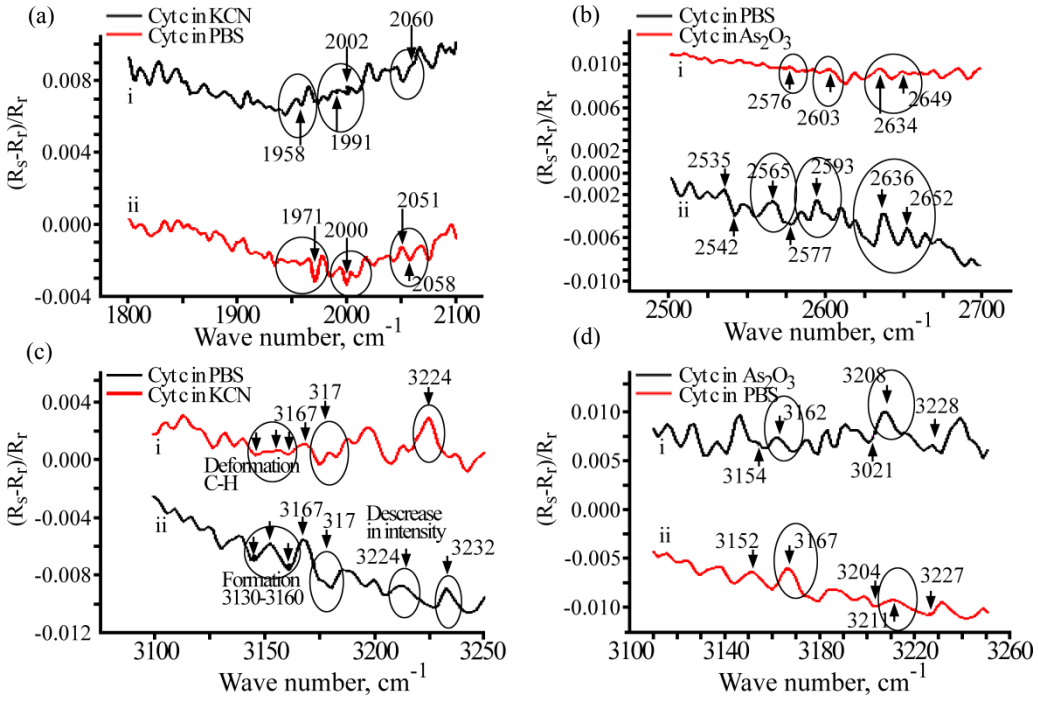

Fig. 6. SNIFTIR of GC/*cyt c*: (a), (b), (c), (d) – in PBS (pH = 7): (a), (c) – in 0.05 mM KCN, and (b), (d) – in 0.05 mM As_2O_3.

SNIFTIR spectroscopy

Cyt c was drop coated onto a GC disk electrode of the diameter of 70 mm and interferograms were recorded using the Ag/AgCl reference electrode and the Pt wire counter electrode. Spectra were measured at potentials from +500 mV to -500 mV, at 100 mV intervals, by Fourier transformation after averaging 300 interferograms acquired at each potential. The CaF_2 window was used in order to limit the influence of the solvent on the spectra. IR spectra were normalized with respect to the reference spectrum, collected at -500 mV, and are displayed as $\Delta R/R$ [(Rs-Rr)/Rr] different spectra. Therefore, SNIFTIRS spectra obtained in this way contain only information of the molecular changes resulting from the modification of the protein. Potentials of -200 mV, -300 mV and -400 mV were closely analysed, since the reductive peak potential in CV and SWV were observed in this region in our earlier work (*18*) and as observed in CV above (Fig. 5b).

The SNIFTIR technique was employed to study the chemical change of the adsorbed *cyt c* and of analytes KCN and As_2O_3 at the GC and Pt electrodes surfaces as a function of applied potential. The vibrational spectra were used to study (i) the dependence of the band intensity on the surface coverage, (ii) the orientation of a molecule at the surface, and (iii) the stability of adsorbed molecules at negative potentials. The SNIFTIR spectra in Fig. 6 were acquired using the reference potential (SCE) – 500 mV where *cyt c* molecules are adsorbed from the electrode surface. The absorption bands corresponding to the adsorbed species should have a negative sign. The bands corresponding to the adsorbed species should also be frequency shifted with respect to the bands of the solution species either due to the Stark effect or due to a different chemical environment of adsorbed molecules. The upward spectra show a decrease in absorption (positive sign) and downward spectra show an increase in absorption (negative sign).

In Fig. 6c,d, the SNIFTIR spectrum for E = -0.03V displays essentially strong bands at 3130–3160 cm^{-1} corresponding to the C-H and O-H (carboxylic acids) stretch. The bands are observed from *cyt c* in PBS and in KCN and As_2O_3. Deformation and decrease in intensity of bands occurs at these values. This decrease in intensities and deformation of bonds/bands is due to the binding event that is taking place between the protein and the analyte. Opposite charges between analyte and protein results in strong binding interaction. At higher wave numbers of 3100–3200 cm^{-1} (N-H) the binding event increases as the upward and downward bands decrease in intensities (Fig. 6c,d). Figure 6a and b also shows spectra of GC/*cyt c* in PBS and in KCN and As_2O_3 at waves of 1800–2700 cm^{-1}. The bands occurring at those wave numbers are in good agreement with the bands recorded for GC/*cyt c* in normal FTIR. The C-H, C=N and the S-H bands (2092 and 2715 cm^{-1}) in FTIR correspond to the SNIFTIR bands at 2058 and 2650 cm^{-1}. These bands are associated with S-H and C≡N stretches at 2550 cm^{-1} and 2092 cm^{-1}. They are blue shifted by 30–50 cm^{-1} with respect to the bands measured in the FTIR mode for *cyt c*. In Fig. 6b, spectrum (i) intense peaks are observed at 2652, 2636, 2593, 2565 cm^{-1} (S-H, C-O and C-H), which decrease in intensities. The same bands are observed in spectrum (ii), whose intensity

decreases at 2642, 2654, 2603, 2576 cm^{-1}. These latter bands show a shift of 10–14 cm^{-1} with respect to the bands observed in spectrum (i). This behavior suggests that the potential-induced reorientation of the adsorbed *cyt c* molecule is coupled with a change in their chemical state. The electrons transferred from the amino acids to the metal center (Fe^{3+}) of the protein are blocked, thus causing the molecular structure of the protein to be distorted. This can be due to the analyte, i.e. KCN and As_2O_3, binding on the amino acids side chains. The observed result reveals that there is a bond deformation occurring at the electrode-interface and new bonds are formed. This bond deformation occurs at one of the amino acids that surround the protein, e.g. cysteine. Literature indicated that the peak potential of cysteine is observed at -290 mV and -450 mV when the two cysteine combine due to disulphide bonds (*22–23*). Electrochemical analysis of L-Cysteine was carried out by CV and SWV (Fig. 7).

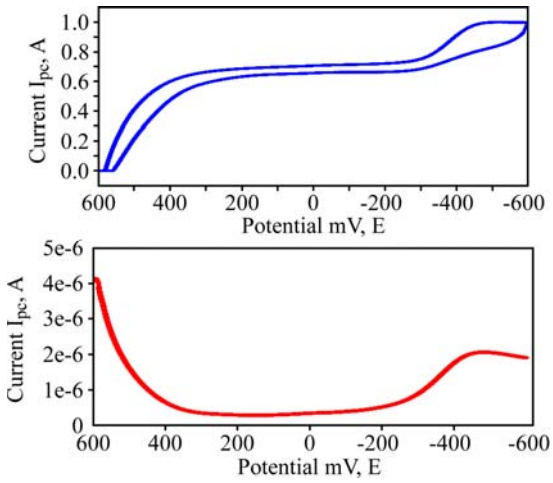

Fig. 7. CV and SWV for cystin at potentials of 600 to -600 mV.

We observed a peak associated with the cysteine reduction at -400 mV, which agrees well with literature (*23–24*). In our previous work the reduction peak potential of cytochrome c was also observed at these potentials using cyclic voltammetry and square wave voltammetry (*18*). Schemes 1 show the binding mechanism of the analytes to the protein.

A number of investigations on the effect of CN- to *cyt c* oxidase, a precursor of *cyt c*, have been carried out to show the inhibition/binding of the protein/enzyme (*27, 28, 29, 30, 31*). We have studied the effect of As^{3+} in our earlier work (18). In our previous work these ligands, i.e. CN- and As^{3+}, were found to interact with the protein at the same potentials. As it was reviewed in literature, cyanide compounds (e.g., KCN), were found to bind to the metal center of the proteins or enzymes (*25*). The CN- ligand binds to Fe^{3+} of the protein reducing it to Fe^{2+} (*27*, *29*). The embedded Fe^{3+}/Fe^{2+} was not observed as the redox for Prussian blue with cytochrome c (*18*). However, As^{3+} was observed to bind to the amino acids of the protein, evidenced by the cysteine peak potential (Fig. 6) at which the binding occurs. This ligand is bound to the amino acids of the protein due to ionic/covalent bonding. Covalent bonds are usually formed between non-metals, with a more electronegative element in the bond attracting a negative charge, thus creating a dipole. In an ionic bond the electrons are not shared but they are held together in the bond by the attraction of the resultant opposite charges. Arsenic can either be bonded to oxygen or to sulphur, due to their electronegativity, hence two routes are shown (Scheme 1). The cation is bound to oxygen first because it is more electronegative than sulphur; hence its dipole moment is smaller. Due to this reason the O-H bond is weaker than the S-H bond, thus making it easy for arsenic to break the O-H bond.

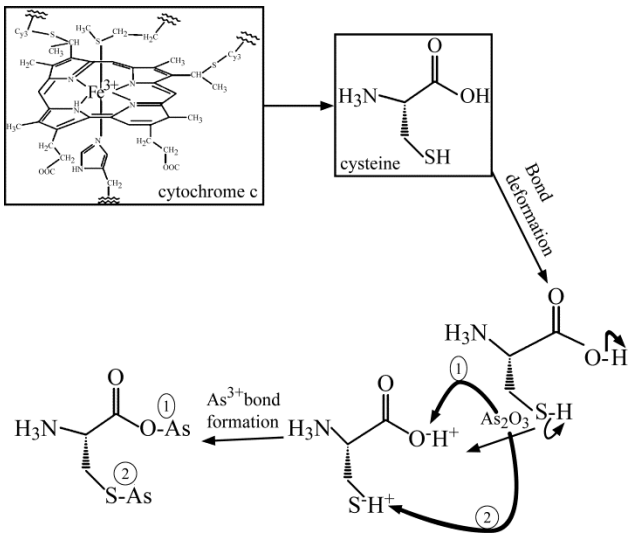

Scheme 1. Schematic representation of arsenic bond formation to cytochrome c amino acid.

CONCLUSION

Spectroscopic (SNFTIR and FTIR) and microscopic (AFM) techniques were used to confirm the native state of the immobilized *cyt c* on the GC and Pt electrodes. FTIR confirmed the bond vibrations of the surface functional groups associated with the protein amino acid backbone; SNFTIR showed the deformation of these functional groups as the protein is electrochemically reduced. These two techniques and the fluorescence spectroscopy confirm the binding of cyanide and arsenic ligands to the protein amino acid (cysteine), observed by a decrease in peak intensities in voltammetry and a change in the structural morphology. Electrochemical methods of CV and SWV proved cysteine to be an amino acid binding site. Based on these findings, a mechanism was proposed for the bond deformation and structural changes within *cyt c*, associated with the biosensor response to the analyte in solution.

ACKNOWLEDGEMENTS

We acknowledge the financial support from the National Research Foundation (NRF), South Africa

and the Organization for the Prohibition of Chemical Weapons (OPCW)

REFERENCES

1. Lee K.-P., Gopalan A.I., and Komathi S. Direct Electrochemistry of Cytochrome c and Biosensing for Hydrogen Peroxide on Polyaniline Grafted Multi-walled Carbon Nanotube Electrode. *Sensor Actuat B-Chem*. 2009, **141**, 518–525.
2. Domènech Ò., Redondo L., Picas L., Morros A., Montero M.T., and Hernández-Borrell J. Atomic Force Microscopy Characterization of Supported Planar Bilayers that Mimic the Mitochondrial Inner Membrane. *J Mol Recognit.* 2007, **20**, 546–553.
3. Jiang X., Wang Y., Qu X., and Dong S. Surface-enhanced Resonance Raman Spectroscopy and Spectroscopy Study of Redox-induced Conformational Equilibrium of Cytochrome c Adsorbed on DNA-modified Metal Electrode. *Biosens Bioelectron*. 2006, **22**, 49–55.
4. Dwivedi U.N., Singh P., Pandey V.P., and Kumar A. Structure-function Relationship Among Bacterial, Fungal and Plant Laccases. *J Mol Catal B-Enzym*. 2011, **68**, 117–128.
5. Whitesides G.M., Yang J., Ferrigno R., and Xiaoxi Chen. Redox Properties of Cytochrome c Adsorbed on Self-Assembled Monolayers: A Probe for Protein Conformation and Orientation. *American Chemical Society*. 2002, **18**, 7009–7015.
6. Boussaad S., Tao N.J., and Arechabaleta R. Structural and Electron Transfer Properties of Cytochrome c Adsorbed on Graphite Electrode Studied by in Situ Tapping Mode AFM. *Chem Phys Lett.* 1997, **280**, 397–403.
7. Hobara D.I., S. Kakiuchi T. Preferential Adsorption of Horse Heart Cytochrome c on Nanometer-Scale Domains of a Phase-Separated Binary Self-Assembled Monolayer of 3-Mercaptopropionic Acid and 1-Hexadecanethiol on Au(111). *Nano Lett.* 2002, **2**, 1021–1025.
8. Lee J.B.K., D.-J., Chio J.-W., Koo K. Direct Electrochemistry of Cytochrome c and Biosensing for Hydrogen Peroxide on Polyaniline Grafted Multi-walled Carbon Nanotubes Electrodes. *Sci Eng*. 2004, **24**, 79–81.
9. Ding X.-D.L.J., Hu J., Li Q. Cytochrome c Self-assembly on Alkanethiol Monolayer Electrodes as Characterized by AFM, IR, QCM, and Direct Electrochemistry. *Anal Biochem*. 2005, **339**, 46–53.
10. Beatrice Bonanni, D.A., Laura Andolf i, Anna Rita Bizzarri, Ines Delfino. Salvatore Cannistraro Yeast Cytochrome c on Gold Electrode: a Robust Hybrid System for Bio-nanodevices. *Biophysics and Nano-science*, 2004. **10**, 574–576.
11. Desbois A. Resonance Raman Spectroscopy of c-type Cytochromes. *Biochimie*. 1994, **76**, 693–707.
12. Robert A. Copeland, T.G.S. Ultraviolet Resonance Raman Spectra of Cytochrome c Conformational States. *Biochemistry*, 1985. **24,** 4960–4968.
13. Oh S.Y., Park J.-K., Ko C.-B., and Choi J.-W. Patterning of Photosensitive Polyimide LB Film and its Application in the Fabrication of Biomolecular Microphotodiode Array. *Biosens Bioelectron.* 2003, **19**, 103–108.
14. Choi J.-W., Nam Y.-S., Kong B.-S., Lee W.H., Park K.M., and Fujihira M. Bioelectronic Device Consisting of Cytochrome c/poly-l-aspartic Acid Adsorbed Hetero-Langmuir–Blodgett Films. *J Biotechnol.* 2002, **94**, 225–233.
15. David Hvasanov A.F.M., Daniel C.G., Mohan Bhadbhadeb and Pall Thordarson. Optimising the Synthesis, Polymer Membrane Encapsulation and Photoreduction Performance of Ru(II)- and Ir(III)-Bis(terpyridine) Cytochrome c Bioconjugates. *Org. Biomol. Chem*. 2013. **11**. 4602–4612.
16. Ramanavicius A., Kausaite A., and Ramanaviciene A. Enzymatic Biofuel Cell Based on Anode and Cathode Powered by Ethanol. *Biosens Bioelectron.* 2008, **24**, 761–766.
17. Mai C. Optimising the Purification of Terpyridine-Cytochrome c Bioconjugates. *J Sci.* 2009, **36**, 236–246.
18. Fuku X., Iftikar F., Hess E., Iwuoha E., and Baker P. Cytochrome c Biosensor for Determination of Trace Levels of Cyanide and Arsenic Compounds. *Anal Chim Acta*. 2012, **730**, 1–20.
19. Hart C.J., Leslie R.B., Davis M.A.F., and Lawrence, M.G.A. The Interaction between Cytochrome c and Purified Phospholipids. *BBA-Biomembranes*. 1969, **193**, 308–318.
20. Esteve-Núñez A., S.J., Visconti P., Lovley DR., Fluorescent Properties of c-type Cytochromes Reveal their Potential Role as an Extracytoplasmic Electron Sink in Geobacter Sulfurreducens. *Environ Microbiol*, 2007. **10**, 497–505.
21. Chou J., Qu X.G., Lu T.H., Dong S.J., and Wu Y. The Effect of Solution pH on Synchronous Fluorescence Spectra of Cytochrome c Solutions. *Microchemical Journal*. 1995, **52**, 159–165.
22. Chen H., Ma X., Fan D., Luo Y. e., Gao P., and Yang C. Influence of L-Cysteine Concentration on Oxidation-reduction Potential and Biohydrogen Production. *Chinese J Chem Eng*. 2010, **18**, 681–686.
23. Jocelyn P.C. The Standard Redox Potential of Cysteine-Cystine from the Thiol-Disulphide Exchange Reaction with Glutathione and Lipoic Acid. *Eur J Biochem*. 1967, **2**, 327–331.
24. Sela M.L.S. The Reformation of Disulfide Bridges in Proteins. *Biochim Biophys Acta*. 1959, **36**, 471–478.
25. Su L. Characterization of Cyanide Binding to Cytochrome C Oxidase Immobilized in Electrode-supported Lipid Bilayer Membranes. *J Electroanal Chem*. 2005, **581**, 241–248.
26. Whitesides Y.J., Ferrigno R., and Xiaoxi C. Redox Properties of Cytochrome c Adsorbed on Self-Assembled Monolayers: A Probe for Protein Conformation and Orientation. *American Chemical Society*. 2002, **18**, 7009–7015.

27. Stark GR., Stern K.A.A., Yoo J. Cleavage at Cysteine after Cyanylation. *Method Enzymol*. 1977, **2**, 129–132.

28. Zhao G.C., Stern K. Direct Electrochemistry of Cytochrome c on a Multi-walled Carbon Nanotubes Modified Electrode and its Electrocatalytic Activity for the Reduction of H_2O_2. *Electrochem Commun*. 2005, **7**, 256–260.

29. Heather B. Leavesley, L.L., Krishnan Prabhakaran, Joseph L. Borowitz and Gary E. Isom. Interaction of Cyanide and Nitric Oxide with Cytochrome c Oxidase: Implications for Acute Cyanide Toxicity. *Toxicol. Sci*, 2008. **101,** 101–111.

30. Nůsková H.M.V., Drahota Z., Houštěk J. Cyanide Inhibition and Pyruvate-induced Recovery of Cytochrome c Oxidase. *Bioenerg Biomembr*. 2010, **42**, 395–403.

31. Antonini E., Brunori M., Greenwood C. and Malmstrom B.G., Rotilio G.C. The Interaction of Cyanide with Cytochroine Oxidase. *Eur J Biochem*. 1971, **23**, 396–400.

Received 07.05.13

Реферат

Было проведено электрохимическое, спектроскопическое и микроскопическое исследование цитохрома *C* и его иммобилизации с использованием двух электродов: стекловидного угольного (GC) и платинового (Pt). Поведение цитохрома *C* изучалось с использованием цианида и мышьяка как эталонных соединений для такого типа изменений. Для характеристики протеина в связанном состоянии и для подтверждения того факта, что он не был денатурирован при связывании на заранее обработанных электродах, упомянутых выше, были использованы такие методы, как: инфракрасная спектроскопия с преобразованием Фурье для границы раздела с нормализованным вычитанием фона (SNIFTIR), флюоресценция, электрохимический анализ, ИК спектроскопия с Фурье-преобразованием (FTIR), а также атомно-силовая микроскопия (AFM). Сферическая морфология связанного протеина, типичная для природного цитохрома *C*, была определенна с помощью AFM. Связывание протеина прослеживалось как снижение пикового тока, используя вольтамперометрию. Кроме того, было проанализировано снижение интенсивности излучения при флуоресценции в растворе, при применении FTIR и SNIFTIR. Флюоресценция и AFM продемонстрировали наличие процесса связывания белка с аналитами. Это было подтверждено также спектроскопиями FTIR и SNIFTIR, что свидетельствует о том, что процесс связывания происходит в боковой цепи аминокислотного остатка белка.

Ключевые слова: токсичность, цитохром С, платиновый электрод, стекловидный угольный электрод.